



HAL
open science

Waves at the electron plasma frequency associated with solar wind magnetic holes: STEREO/Cluster observations

Carine Briand, J. Soucek, Pierre Henri, André Mangeney

► To cite this version:

Carine Briand, J. Soucek, Pierre Henri, André Mangeney. Waves at the electron plasma frequency associated with solar wind magnetic holes: STEREO/Cluster observations. *Journal of Geophysical Research Space Physics*, 2010, 115, pp.12113. 10.1029/2010JA015849 . hal-03730566

HAL Id: hal-03730566

<https://hal.science/hal-03730566>

Submitted on 22 Aug 2022

HAL is a multi-disciplinary open access archive for the deposit and dissemination of scientific research documents, whether they are published or not. The documents may come from teaching and research institutions in France or abroad, or from public or private research centers.

L'archive ouverte pluridisciplinaire **HAL**, est destinée au dépôt et à la diffusion de documents scientifiques de niveau recherche, publiés ou non, émanant des établissements d'enseignement et de recherche français ou étrangers, des laboratoires publics ou privés.

Copyright

Waves at the electron plasma frequency associated with solar wind magnetic holes: STEREO/Cluster observations

C. Briand,¹ J. Soucek,² P. Henri,^{1,3} and A. Mangeney¹

Received 21 June 2010; revised 7 September 2010; accepted 15 September 2010; published 29 December 2010.

[1] Magnetic depressions are common structures of the interplanetary medium. These magnetic holes can be just isolated dips of the amplitude of the field or they can be associated with discontinuities in the field orientation (tangential or rotational). Electrostatic waves at the plasma frequency (Langmuir waves) are often observed in these magnetic structures. The aim of the present paper is to provide the main characteristics of these waves and to propose a mechanism to explain their formation. The study is based on a statistical analysis of observations performed by STEREO (between March 2007 and August 2009) and Cluster (between 2002 and 2005) when each mission was in the free solar wind. Complementary information is provided by the two missions through the different instrumental configurations. We first provide new characteristics of the waves (polarization, energy, spectrum, occurrence). We then show that the occurrence of Langmuir waves activity inside a hole is closely linked to the presence of a significant electron strahl outside the hole. Finally, we propose a scenario for the generation of the Langmuir waves inside the holes.

Citation: Briand, C., J. Soucek, P. Henri, and A. Mangeney (2010), Waves at the electron plasma frequency associated with solar wind magnetic holes: STEREO/Cluster observations, *J. Geophys. Res.*, 115, A12113, doi:10.1029/2010JA015849.

1. Introduction

[2] Langmuir waves modes are electrostatic waves close to the plasma frequency. They have been intensively studied in relation with type III radio bursts and in the Earth bow shock environment to understand the interactions of solar wind with the magnetosphere. Langmuir waves (LWs) are also observed in magnetic holes. In this paper we report recent observations of Langmuir waves in magnetic holes, providing new constraints to the models of wave generation and to physical conditions inside magnetic holes.

[3] Magnetic holes are commonly observed in space environment since the early flight of Pioneer 6: in the solar wind [Turner *et al.*, 1977; Winterhalter *et al.*, 1994; Lin *et al.*, 1996], in the Earth's magnetosheath [Cummings and Coleman, 1968; Luehr and Kloecker, 1987; Treumann *et al.*, 1990], in the cometosheath [Russell *et al.*, 1987], in the plasma behind interplanetary shocks, and in the heliosheath [Burlaga *et al.*, 2007]. These magnetic depressions can be either isolated structures not related to any particular change in the B -field direction (they are then called *linear holes*) or associated with directional discontinuities (DD) of the magnetic field.

[4] Burlaga *et al.* [1969] distinguished several classes of magnetic holes according to their duration: meso-scale (from a few days to 1 h), micro-scale (from 1 h to 1 min), and kinetic scale (less than 1 min). They suggested that larger holes are governed by hydromagnetic processes, while kinetic theory must be considered to explain the very short magnetic depressions, the size of the structures being of the order of the proton gyroradius. Several studies, using different selection criteria of the magnetic holes, showed that the size of the holes follows a power law, eventually with a break at about 20–40 s [Fränz *et al.*, 2000; Stevens and Kasper, 2007]. This change of scaling suggests that different processes indeed govern large and small structures.

[5] In spite of numerous observations, the question of the origin of the magnetic holes is still puzzling: Are they generated near the Sun and then convected by the solar wind or are they formed locally in the interplanetary space? The presence of magnetic dropouts can affect the transport properties of the particles and the study of magnetic holes and discontinuities can therefore provide information on the large scale structure of the solar wind.

[6] Burlaga and Lemaire [1978] first showed that magnetic holes are pressure equilibrium structures, solution of the Maxwell-Vlasov equations. In situ plasma measurements have confirmed this statement [Winterhalter *et al.*, 1995; Neugebauer *et al.*, 2001; Zurbuchen *et al.*, 2001; Stevens and Kasper, 2007]. They also suggested that magnetic holes could result from an adiabatic pressure response (diamagnetic) of the plasma to a local enhancement of the kinetic pressure. More recently Buti *et al.* [2001] and Tsurutani *et al.*

¹LESIA, Observatoire de Paris, CNRS, UPMC, Université Paris Diderot, Meudon, France.

²Department of Space Physics, Institute of Atmospheric Physics, ASCR, Prague, Czech Republic.

³Also at Dipartimento di Fisica, Università di Pisa, Pisa, Italy.

[2002] proposed that diamagnetic effects could also result from an energization of protons.

[7] Langmuir waves are often excited within magnetic holes. Using data from the URAP instrument on board of ULYSSES, *Lin et al.* [1996] showed the correlation between the electric field power spectrum peaks and the presence of directional discontinuity in magnetic field. In their data set 9% of magnetic discontinuities displayed Langmuir waves activity, but this percentage increased to more than 30% when considering discontinuities associated with a large dip in field intensity. The waves were usually observed at the edges of the holes, that is, where the magnetic gradient is large. Thus, they concluded that the amplitude of magnetic field depression gradient, rather than the amplitude of the holes itself, is a key parameter for the development of Langmuir waves. They also showed that currents generated at magnetic field discontinuities play little role in the excitation of LWs. However, they could not give any details on the waveforms.

[8] Studying the dependence of the LW activity with the heliographic latitude, *MacDowall et al.* [1997, 2001, 2003] reached the following conclusions:

[9] 1. The intensity of the electric field is much higher outside a band of $\pm 20^\circ$ in latitude;

[10] 2. At high latitude, the wave activity is more likely observed in magnetic holes or other magnetic field discontinuities;

[11] 3. The probability of wave activity is higher outside the streamer belt than inside (magnetic holes are more common in the high-latitude solar wind); and

[12] 4. The electric field intensity is higher closer to the sun and shows a tendency to decrease with the distance to the Sun (but also a more surprising increase seems to occur at about 5AU).

[13] All the proposed mechanisms for the formation of magnetic holes are adiabatic, thus very slow. The presence of high-frequency electrostatic waves inside these magnetic dips is thus puzzling. Indeed, Langmuir waves usually require time-dependent fluctuations of the electron distribution function, hardly compatible with a slow formation of magnetic holes. In this study we present new observations of *E*-field waveforms and electron distribution functions providing clues to the understanding of the formation of these waves and reveal new properties of the magnetic holes themselves.

2. Instrumentation

[14] For the present study, we shall use two independent sets of magnetic hole observations, coming from two space missions: STEREO and Cluster.

[15] The STEREO observations are restricted to the ecliptic plane at a distance of about 1 AU from the Sun but cover a large longitudinal extension at large distances from the Earth. The data considered here span over the period 1 February 2007 to 31 August 2009. During this period of time, the Sun was very quiet. The two STEREO S/C were in the free solar wind (except for a short period in March 2007 when STEREO-B reached the flank of the magnetopause). The following data are used: (1) Three-component electric field waveforms of 130 ms duration from the Time Domain

Sampler (TDS) mode of the WAVES instrument [*Bougeret et al.*, 2008]; (2) 8 Hz magnetic field (in spacecraft coordinates) measurements, pitch angle electron distribution, and electron temperature from IMPACT/SWEA [*Luhmann et al.*, 2008; *Sauvaud et al.*, 2008]; (3) 1 min average solar wind bulk velocity and proton temperature from PLASTIC [*Galvin et al.*, 2008].

[16] The plasma thermal noise (“plasma line”) is hidden by the impact noise prohibiting the use of the thermal noise spectroscopy to deduce the electron density. The peak frequency of the Langmuir waves is used instead.

[17] The TDS instrument performs on-board selection of waveform snapshots that are transmitted to the ground if their amplitude is larger than a given threshold. The waveform data are therefore restricted to a limited number of the most intense wave events encountered by the spacecraft (typically less than 100 per day). Therefore, the absence of wave measurements in a magnetic hole does not necessarily mean that the waves were indeed absent. This is important to keep in mind when interpreting the STEREO data presented later in this article.

[18] Unlike STEREO, the Cluster spacecraft orbit the Earth and spend only a small part of their orbit in the unperturbed solar wind. Because we can only consider these intervals in our analysis, care had to be taken to ensure that the spacecraft were located sufficiently far from the foreshock region and the measurements were not perturbed by foreshock electrons and associated waves. The foreshock edge location was calculated from a model by *Cairns et al.* [1997] using local magnetic field and plasma data measured by the same Cluster spacecraft and only measurements further than 1 Earth radius from the model foreshock edge were considered. Furthermore, Cluster electric field spectrograms for the selected events were visually scanned for signatures of foreshock crossing, easily recognized by long continuous emission of intense narrowband waves. These intervals were excluded from the data set.

[19] In this study we used the following Cluster data: (1) Magnetic field vector sampled at 5 Hz from the flux-gate magnetometer (FGM) [*Balogh et al.*, 2001]; (2) high-frequency electric field from the Whisper instrument [*Décroux et al.*, 1997] (the spectra cover the frequency range from 2 to 80 kHz and are available approximately once in 2 s); (3) high-frequency electric field waveforms from the wide-band (WBD) instrument [*Gurnett et al.*, 1997] sampled at 220 kHz and available in the form of 10 ms snapshots taken regularly every 80 ms; (4) pitch angle distributions provided by the PEACE electron instrument once or twice per satellite spin [*Johnstone et al.*, 1997].

[20] We used data from years 2002, 2004, and 2005. We restricted the search for suitable events to the periods when the Cluster apogee was on the day side of the Earth (December to May).

3. Data Selection and Classification of Magnetic Field Structures

[21] Due to instrumental constraints the selection of the events was performed differently for the STEREO and Cluster data set; each data set will be used to address different questions.

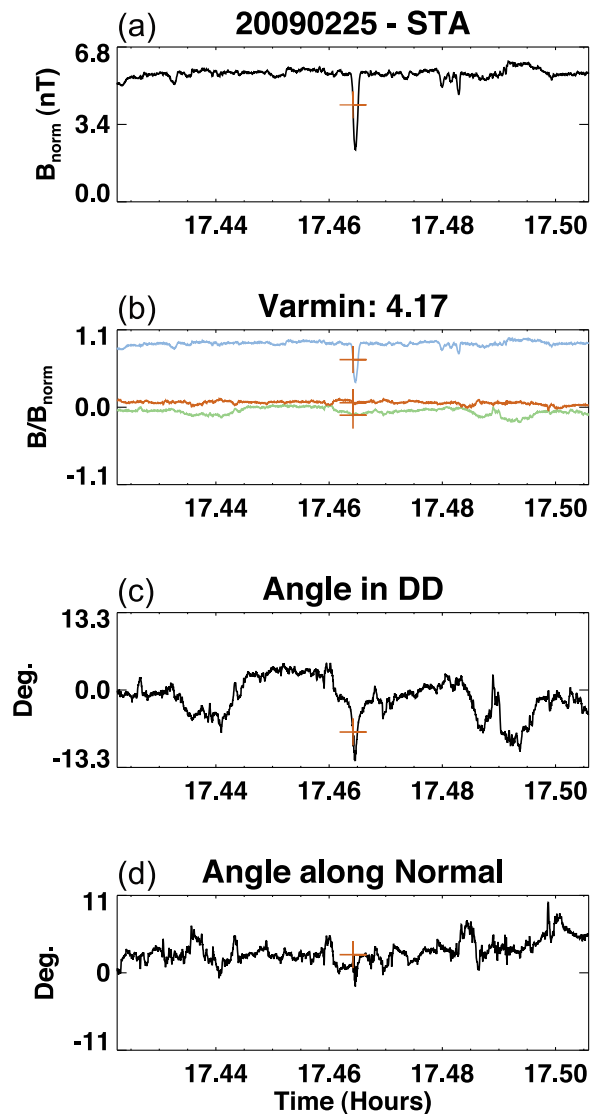


Figure 1. Example of linear magnetic hole. (a) Norm of the B field (in nanoteslas). (b) B field in the variance frame, normalized to the maximum value of the norm of B (in blue: the maximum variance, in red the minimum variance, in green the intermediate variance). “Varmin” indicates the ratio of the intermediate to maximum eigenvalue. (c) The rotation angle in the plane of the discontinuity. (d) The rotation angle perpendicular to the plane of the discontinuity (along the maximum variance axis). For Figures 1a–1d, the red crosses indicate the location of the wave activity.

3.1. STEREO Data Set

[22] Only a limited number of on-board selected TDS waveforms are transmitted by STEREO. Thus, we choose to select the magnetic configurations from the list of all TDS Langmuir wave observations in the analyzed period. So no criteria are applied on the selection of the magnetic configuration, except the presence of a significant E -field activity (i.e., a power spectrum at the Langmuir peak greater than 10 times the background level) above 5 kHz. Langmuir waves events associated with type II and type III emissions

have been removed. The magnetic field configuration is plotted in a 5 min window for each interval of observed wave activity.

[23] The identification of the magnetic structures in terms of “Linear” or “Directional” holes is based on the following criteria: (1) linear hole: isolated depression of the norm of the magnetic field with a field rotation lower than about 10° (Figure 1); and (2) direction discontinuities: presence of a magnetic depression and together with a large rotation either on the plane of discontinuity (tangential) and/or in the plane perpendicular (rotational). In the following, we do not distinguish between the two types of DD (Figure 2).

[24] The instantaneous B -field rotation is defined as:

$$\sin(\theta) = |B(t)B(t+1)| / |B(t)| \times |B(t+1)| \quad (1)$$

where B is the magnetic field vector at time t and $t+1$. This procedure allows to follow without ambiguity the rotation

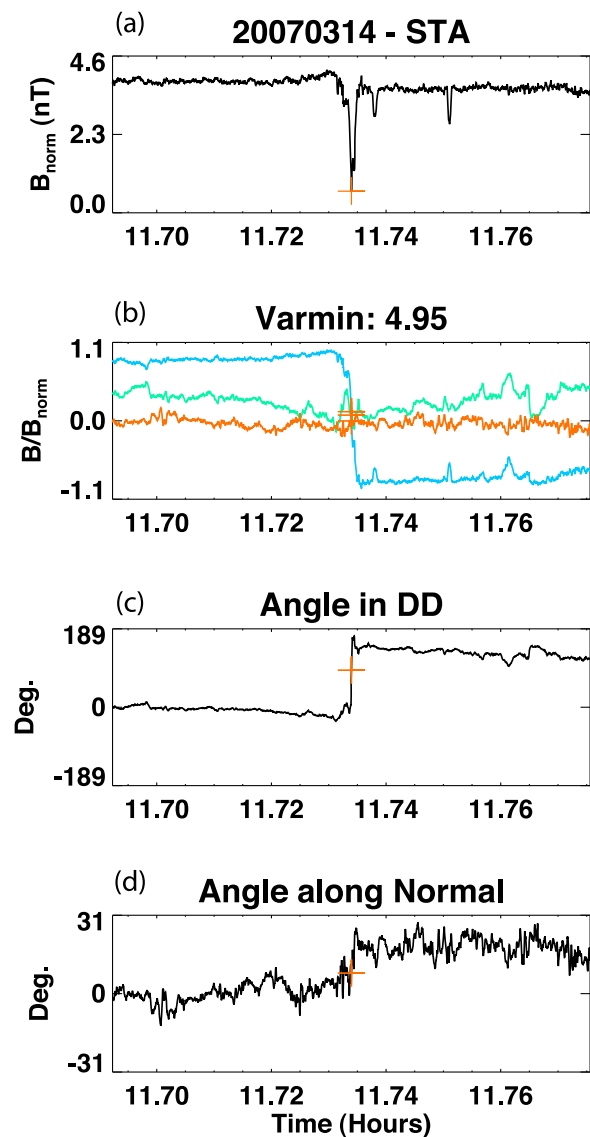


Figure 2. Same as in Figure 1 for a magnetic hole associated with directional discontinuities.

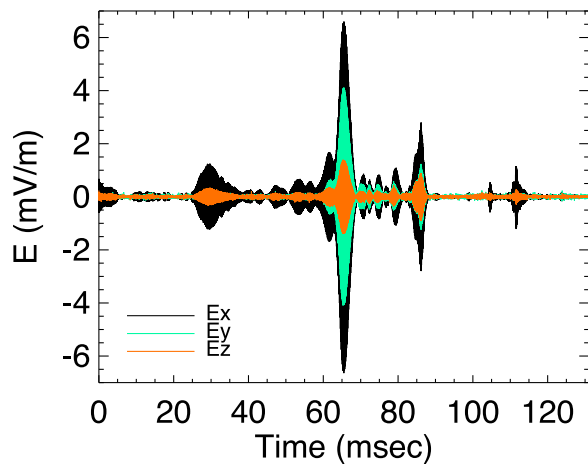


Figure 3. Example of electric waveforms inside a linear magnetic hole along three spatial directions (as defined by equation 2). Changes in the polarization can be appreciated by the variations of the relative amplitude along the three components inside short time wave packets. From S/WAVES.

of the field vector with time since the rotation remains small between two successive times. The magnetic field is expressed in minimum variance coordinates (maximum, intermediate, and minimum eigenvectors) to identify rotation in the plane of the discontinuity and perpendicular to it.

[25] We have chosen to identify visually the magnetic discontinuities since no exact criteria are valid: linear holes are usually associated with rotation angles smaller than 10° [Winterhalter *et al.*, 1994] to 15° [Zhang *et al.*, 2008], although no arguments are provided for the justification of these specific threshold values. Moreover, the Langmuir events are often located in dips embedded in a noisy magnetic background. The identification of the true nature of the hole with an automatic procedure is thus hazardous and would require a visual control anyway.

[26] From 1 February 2007 to 31 August 2009, 691 Langmuir events have been detected (311 from STEREO-A and 380 from STEREO-B) and are distributed among 358 distinct magnetic configurations. We restrict our study to the well-identified cases of linear holes and directional discontinuities that represent only 146 configurations. Linear holes represent 38% of the remaining samples and DD 62%. Note that a large majority of magnetic configuration has been rejected. They correspond to cases (i) where no magnetic depression was observed and (ii) where the edges of the magnetic depression were impossible to identify unambiguously because they are embedded in a rapidly varying background. The characterization of the waves in such peculiar environment will be the subject of another work.

3.2. Cluster Data Set

[27] Since the electric field data from the Whisper instrument are available almost continuously, the search for magnetic hole events in Cluster data was performed in a different way. An automatic algorithm was used to select free solar wind intervals in the Cluster data for the day-side seasons of 2002, 2004, and 2005, determined by visual inspection of the data and then manually searched for mag-

netic hole events. Magnetic holes were defined as localized decreases in magnetic field magnitude of at least 20% observed at timescales from few seconds to 5 min surrounded by intervals of nonfluctuating magnetic field. This semiautomatic procedure yielded a data set of 65 magnetic hole events.

[28] Although four spacecraft measurements are available for most events, data from only one spacecraft were included in the statistics for each hole. As the PEACE instrument is normally operated only on one spacecraft during solar wind passes, we usually selected the reference spacecraft based on PEACE data availability.

[29] The observed holes were included in the data set regardless of the presence of associated Langmuir waves; the data set therefore includes a significant fraction of holes without observed wave activity and can be used for statistical investigation of factors correlated with wave occurrence (section 4.1). The holes were classified into “linear” and “directional” according to the same criteria described above for the STEREO data.

4. Properties of Observed Waves

[30] The waveforms reveal the very bursty nature of the electric field (Figure 3). The frequency peak of the different short time wave packets inside the TDS events vary by ± 2 kHz, resulting in a broadening of the peak in the power spectrum around the primary wave frequency. The modulation can be a signature of (i) waves being generated by low-energy warm electron beams, (ii) the transient and fluctuating nature of the electron beam responsible for wave generation, (iii) inherent plasma density fluctuations, or (iv) electron trapping in the potential field of the waves [Muschiatti *et al.*, 1994]. Thermal and Doppler shift broadening appear to be second order effects (about a few hundred hertz in the solar wind conditions and beam velocity of about $5 v_{th,e}$).

[31] Owing to the 3-D waveform measurements, we can, for the first time, check the polarization of the waves with respect to the ambient magnetic field. To do so, B and E fields are first projected into the following frame:

$$e_x = B(t_0) / |B(t_0)| \quad (2)$$

$$e_y = e_x \times V_{sw} / |V_{sw}| \quad (3)$$

$$e_z = e_x \times e_y, \quad (4)$$

where $B(t_0)$ stands for the direction of the magnetic field at time t_0 of the beginning of the Langmuir event and V_{sw} the direction of the solar wind (assumed to be in the radial direction). By construction, the B field is along the e_x component.

[32] The tips of the E -field components in the $e_x - e_y$ and $e_x - e_z$ planes follow a curve that is fitted by an ellipse. The eccentricity of the ellipse in each plane serves to infer the type of polarization: A linear polarization implies an eccentricity is close to one in the two planes. The polarization angle $\alpha = \arccos(\cos \xi \cos \phi)$ defines the angle between the main axis of the E -field ellipsoid and the background magnetic field. Here ξ is the angle the projection of the E field in the plane $e_x - e_y$ and ϕ in the plane $e_x - e_z$. This angle α

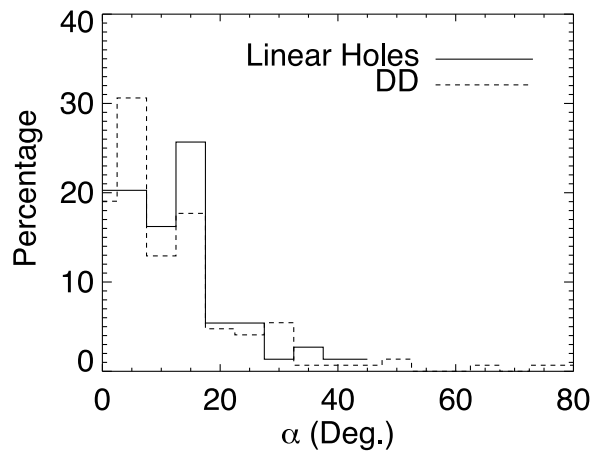


Figure 4. Histogram of the polarization angle α of the waves relative to the B field for linear holes (solid line) and DD (dashed line).

is zero for waves exactly polarized parallel to the magnetic field.

[33] Figure 4 displays the histogram of the angle α for waves inside the two types of holes. Although some of the waves exhibit a clear transverse component, a large majority of the observed waves is clustered in the region of small polarization angles and the polarization is linear (the eccentricity is close to 1). This confirms that the waves are linearly polarized mostly along the direction of the magnetic field. The median value of the polarization angle α is 11° for waves in linear holes and 13° for waves in DD. Thus, the type of B holes does not influence the polarization of the electrostatic waves.

[34] Now, individual wave packets inside a same TDS event of 130 ms often present multiple (still linear) polarization orientations: fluctuations up to 50° of the polarization angle are observed (Figure 5). Several interpretations are possible. If we assume that the waves are pure Langmuir waves (thus aligned with B), then the variations of polari-

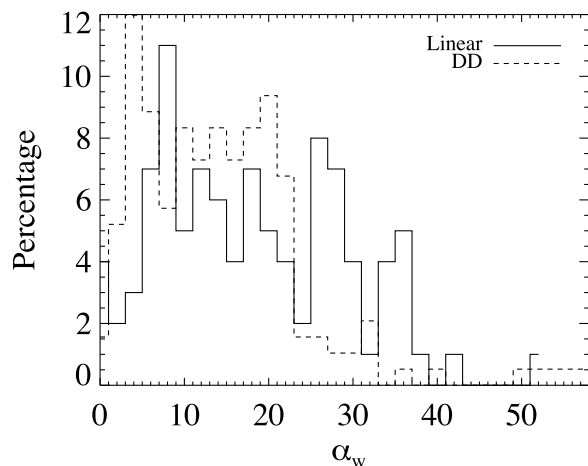


Figure 5. Histogram of the polarization angle α_w relative to B for individual wave packets chosen inside several TDS events.

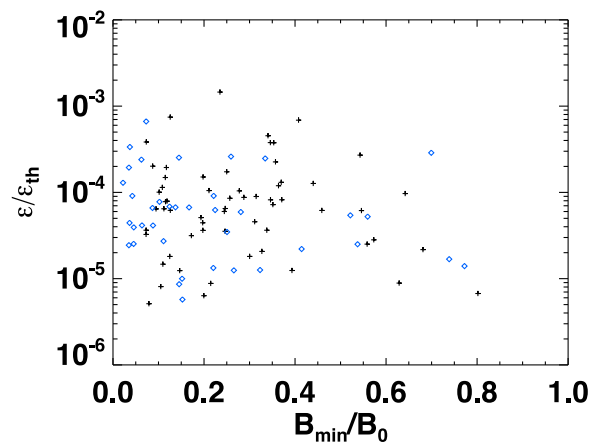


Figure 6. Electric energy of the waves versus hole depth. The energy is expressed in unit of thermal energy. Crosses, linear holes; diamonds, DD.

zation reveal very short time fluctuations of the magnetic field orientation. The second interpretation takes into account the weak magnetization of the plasma. In such a case, the Langmuir dispersion branch is continuously connected to the Z mode, which may lead to oblique propagation of waves close to the plasma frequency. The observed polarization would then be the signature of Z modes as the hole passes by the spacecraft.

[35] The maximum of the wave energy ϵ (normalized to the thermal energy) is shown as a function of the depth of the holes in Figure 6. The thermal energy is evaluated from the electron density deduced from the frequency peak of the Langmuir events and a constant electron temperature of 10^5 K. The energy in the waves is similar in linear and DD (median value of 5×10^{-5}): this is about one order of magnitude lower than the level of Langmuir waves associated to type III bursts [Henri *et al.*, 2009]. The observed energy is poorly correlated to the depth of the holes (Figure 6). The statistics are, however, biased by the small number of shallow holes.

[36] The Cluster data set allows us to characterize the probability of occurrence of Langmuir waves inside magnetic holes. Table 1 shows the number of holes containing Langmuir wave activity and holes without any wave activity for each type of magnetic holes. Despite the small size of the data set, it can be concluded that about half of all observed magnetic holes contain some indication of wave activity.

Table 1. Occurrence of Langmuir Waves in Different Types of Magnetic Holes^a

	All Holes	Linear Holes	Holes With DD
Cluster: Holes with waves	36 (55%)	26 (58%)	6 (50%)
Cluster: Holes with no waves	29 (45%)	19 (42%)	6 (50%)
STEREO: Holes with waves	146	55	91

^aFor the Cluster data set, eight holes fall in the unidentified category (neither linear nor directional). The last row shows the results for the STEREO data set. Note that for the STEREO data, events were identified based on the observation of Langmuir waves.

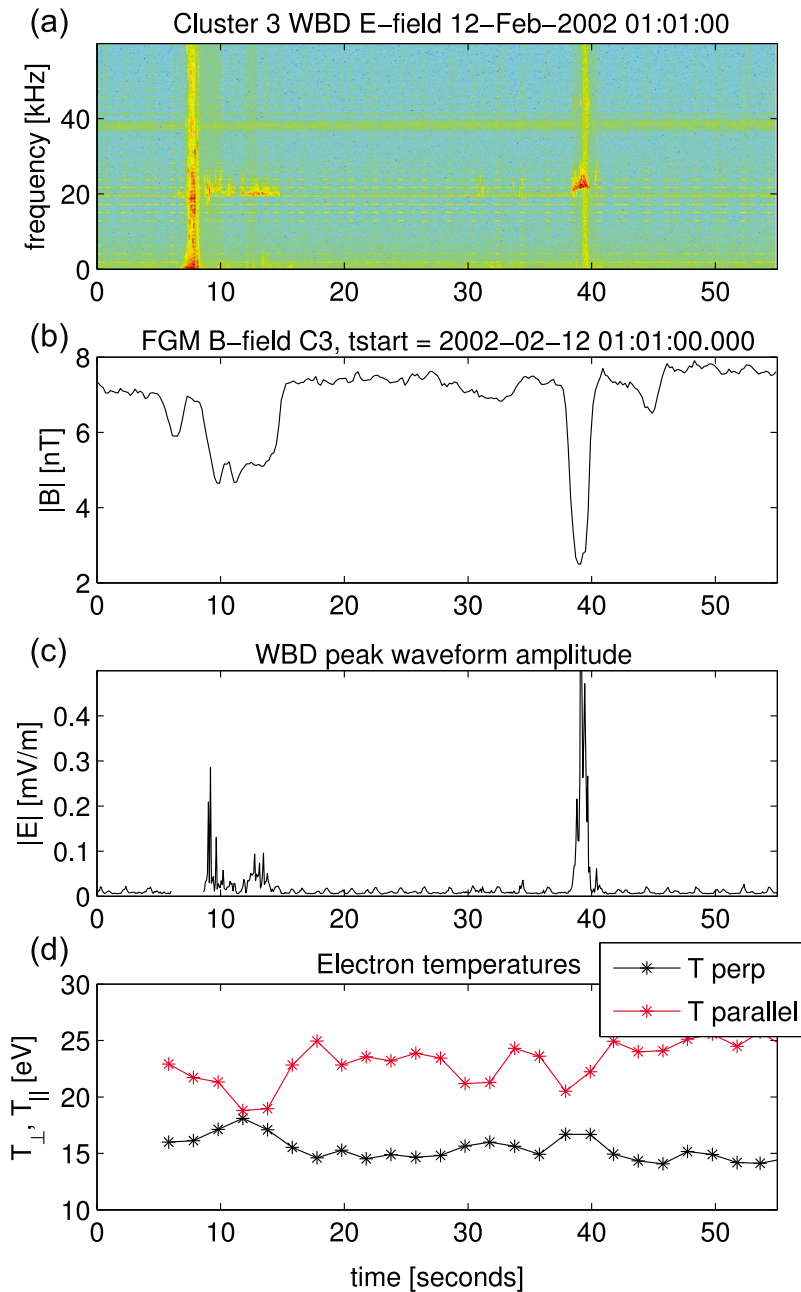


Figure 7. Detailed view of magnetic holes observed by Cluster. (a) Electric field spectrogram (WBD instrument). The strong broadband signature just before the first hole is an instrumental effect (a signature of Whisper resonance sounder sweep). (b) Magnetic field magnitude (FGM). (c) Peak electric field amplitude (WBD). (d) Parallel and perpendicular electron temperature.

This result is roughly consistent with the results of *Lin et al.* [1996].

[37] Also, among the 691 E -field events detected by STEREO, a large number of Langmuir events occur outside magnetic holes. Indeed, only 11% are located inside linear holes and 21% are located in DDs. Note that the larger number of waves inside DD can just result from the larger number of DD detected.

[38] Based on their analysis of Ulysses data, *Lin et al.* [1995] report that the waves are often observed at the

edges of the holes. Our data partly confirm this statement. In several DD, waves occur at the center of the hole. Moreover, in the case of narrower linear holes, Cluster data show that the waves typically fill the entire hole, although an increase in wave amplitude may be observed close to the hole boundary. An example is shown in Figure 7. The figure presents a rare event where a solar wind magnetic hole was observed on Cluster while high resolution electric field data from the WBD instrument were available. The two linear holes (8 and 3 s wide) are clearly associated with bursts of

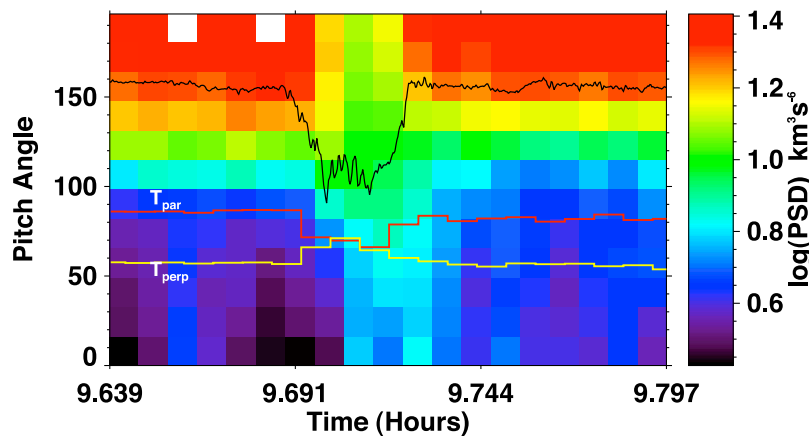


Figure 8. Pitch angle electrons at $E = 257$ eV (0° pitch angle means B -field-aligned particles) with superimposed the magnetic field strength (in black), the electron temperature T_{perp} (in yellow), and T_{par} (in red) for the same time interval. From STEREO.

wave activity at the plasma frequency over the full width of the holes.

5. Electron Distribution

5.1. Isotropization Inside the Holes

[39] The localized decrease in magnetic field modifies the properties of local electron distribution. Cluster and STEREO particle instruments allow us to investigate the change of the electron distribution function inside the magnetic holes. Figure 8 shows an example of electron pitch angle distribution measurements performed by the IMPACT/SWEA instrument of the STEREO spacecraft across a magnetic holes. The data come from a single energy channel of the instrument centered at an energy of 257 eV. At this suprathermal energy, the major contribution to the solar wind electron distribution comes from the field-aligned strahl component, as can be easily seen from the concentration of the distribution around antiparallel pitch angles.

[40] The figure indicates that there is a redistribution in pitch angle of the electrons, revealing an isotropization of the particle distribution inside the hole. The same effect is observed in other energy channels of the instrument and consistently in the data from the PEACE instrument of Cluster (not shown). This isotropization has an obvious effect on the electron temperatures measured by the spacecraft (temperature curves of Figure 8). As the parallel strahl intensity decreases, the parallel temperatures (derived from direct moment integration for electron energies above 45 eV.) strongly decrease and simultaneously the perpendicular temperature displays a moderate increase.

[41] Exactly the same effect is observed on Cluster, where higher time resolution of the measurements (2 or 4 s compared to 30 s on STEREO) allows us to demonstrate this effect even inside relatively narrow linear holes. Figure 7d shows the parallel and perpendicular temperatures estimated from the pitch angle distributions provided by the PEACE instrument (here data from the two sensors LEEA and HEEA were combined to obtain maximum time resolution of half the spin period). The isotropization described

above shows up in this measurement as well. This increase (decrease) of the perpendicular (parallel) temperature inside the holes was already noticed for ions [Fränz *et al.*, 2000; Neugebauer *et al.*, 2001; Tsurutani *et al.*, 2002; Stevens and Kasper, 2007]. This is the first time it is also observed for electrons.

[42] The presence of a magnetic hole therefore leads to a scattering of the strahl and an isotropization of the electron distribution inside the hole. This effect was observed in a number of other events not shown in this article and appears to be relatively common in solar wind holes. A systematic statistical investigation of its occurrence is complicated by a number of instrumental effects associated with particle data and may be the subject of a future study. The measurements presented in the present paper were checked for instrumental effects and possible errors resulting from the rapid change in magnetic field direction during the measurement were ruled out in these cases. The fact that two instruments of different designs on different spacecraft observed the same effect also increases our confidence in the observation.

5.2. Relevance of Suprathermal “Strahl” Electrons

[43] The electron population of the solar wind plasma is known to present strong suprathermal non-Maxwellian features; it is traditionally decomposed into three populations: a bi-Maxwellian thermal “core,” a non-Maxwellian but isotropic “halo,” and a field-aligned “strahl” propagating usually in the anti-sunward direction [Montgomery *et al.*, 1968; Feldman *et al.*, 1975]. In this section we present observations of electron distribution functions associated with magnetic hole events potentially relevant to the mechanism of wave generation. We investigated a possible connection between the presence of the strahl and the occurrence of Langmuir waves inside magnetic holes by using the Cluster data set described in section 3.

[44] The presence of a strahl component was determined by evaluating the asymmetry of observed electron distribution in the solar wind surrounding the hole. A 20 s interval with minimum fluctuation of the magnetic field was chosen from a 2 min time range surrounding the hole. Four subsequent

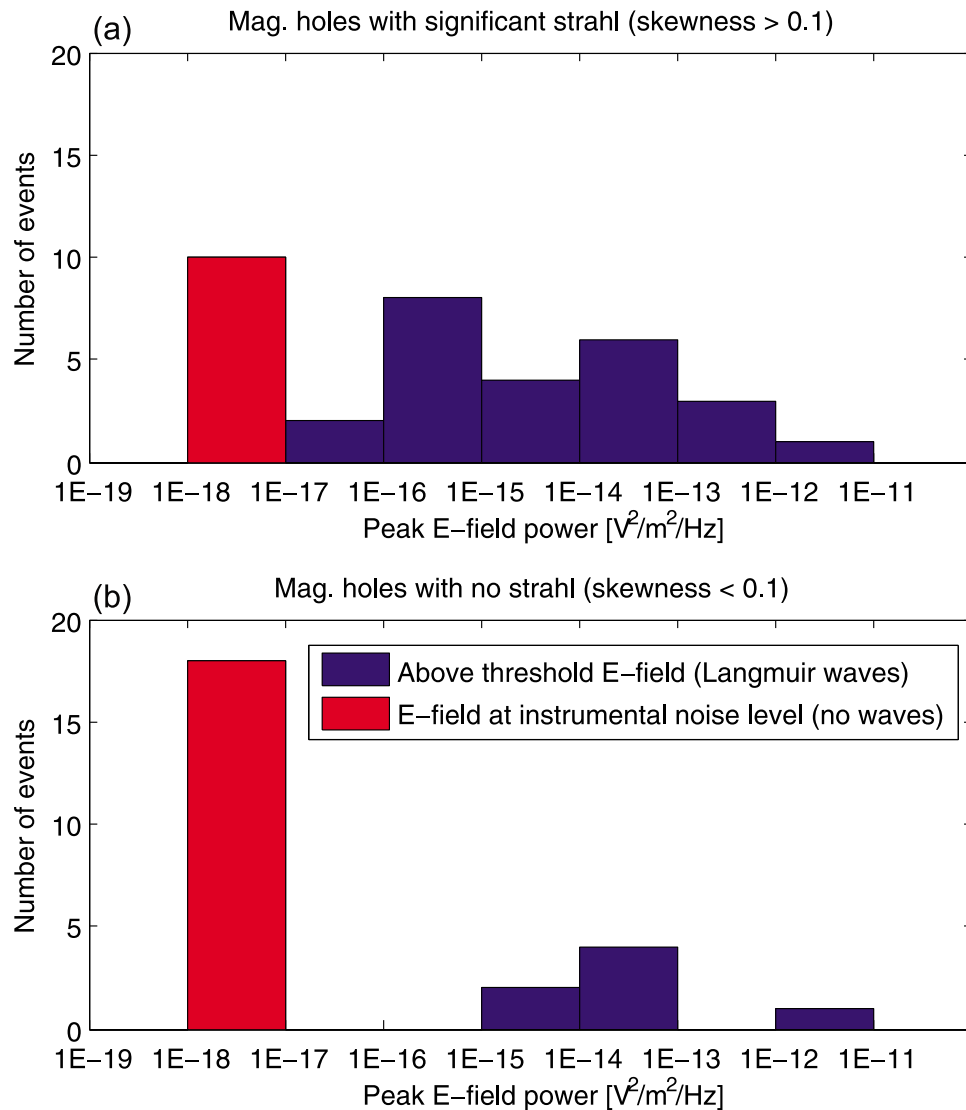


Figure 9. Histogram of the peak wave amplitudes for two groups of solar wind conditions: (a) events when a clear electron strahl is seen in the surrounding solar wind and (b) in absence of strahl in the local solar wind. The red column (power below $10^{-17} \text{ V}^2 \text{ m}^{-2} \text{ s}^{-1}$ is the noise level of the Whisper instrument) corresponds to events with no Langmuir waves. The blue columns correspond to waves of experimentally significant measured amplitudes.

pitch angle distributions captured by the LEEA sensor of PEACE during this interval were averaged together to reduce the effect of relatively low particle counts. Next the averaged pitch angle distribution was integrated over perpendicular velocities yielding a reduced distribution $f(v_{\parallel})$.

[45] When a significant anti-sunward strahl component is present in the solar wind plasma, the reduced distribution will be strongly asymmetric with an enhancement in the anti-sunward half. The presence of a strahl can be therefore easily quantified by calculating the skewness of the reduced distribution:

$$S[f] = \int f(v_{\parallel}) v_{\parallel}^3 dv_{\parallel}. \quad (5)$$

[46] The PEACE instrument provided good electron measurements for 61 events of the 65 magnetic holes in our

Cluster data set. These 61 events were divided into two categories according to the presence of strahl in the background solar wind at the time of their observation. After visual inspection of the distributions, the condition $S[f] > 0.1$ was chosen as a criterion for presence of a significant asymmetry in the distribution and hence significant strahl. From a total of 61 magnetic hole events 39 of them correspond to solar wind with significant strahl and 22 to solar wind with weak or no strahl.

[47] The occurrence of Langmuir waves inside the magnetic holes was investigated in these two groups of holes. The waves were identified by the maximum amplitude of the electric field inside the hole using the integrated electric field wave power data from the Whisper instrument of Cluster (available approximately five times per second). The results of the analysis are shown in Figure 9. The histograms show the distribution of peak wave power inside the holes

for the two groups. Blue columns indicate presence of Langmuir waves.

[48] Clearly, the occurrence of Langmuir waves inside magnetic holes was much higher during events where a strong strahl was present in the solar wind. In the case when no or a very weak strahl was observed in the solar wind plasma (Figure 9b) 17 holes show no wave activity and only 5 present some waves. In the category of events possessing a significant strahl (Figure 9a) the ratio is opposite: 11 holes with no waves and 28 holes with waves.

[49] This statistic shows that the occurrence of Langmuir wave activity inside solar wind magnetic holes is associated with the presence of a significant electron strahl population in the local solar wind. This observation suggests that the strahl likely plays a critical role in the generation of the waves, possibly supplying the suprathermal electrons responsible for the instability. Another possible interpretation that cannot be completely ruled out is that solar wind conditions corresponding to a diminished strahl are not favorable for the excitation of Langmuir waves inside magnetic holes.

6. Wave Generation Mechanism

[50] A likely candidate for the generation mechanism of longitudinally polarized electrostatic waves is the beam plasma instability (“bump on tail”) responsible for similar waves in various environments (e.g., Earth foreshock and type II and type III bursts). Although a bump occurring at some nonzero pitch angle can generate Langmuir waves [Yoon *et al.*, 2000], we shall limit ourselves to the more robust instability criterion requiring a localized positive gradient $\partial f(v_{\parallel})/\partial v_{\parallel} > 0$ in the reduced electron distribution function f , easier to compare with the present low time resolution observations. It is not obvious to explain how such a positive slope in the electron distribution function may be formed in a magnetic hole, especially if one takes into account the fact that linear instability theory shows that “slow beams” (i.e., with velocity such that $v_b \approx v_{te}$) with a beam temperature similar to core electron temperature and density smaller (not necessarily much smaller) than the core plasma density are not sufficient to drive the plasma unstable [Gary, 1985].

[51] Consider the simplest case of a “linear hole” at rest in the solar wind (magnetic holes are generally believed to be nonpropagating structures convected by the solar wind flow [Burlaga and Lemaire, 1978; Winterhalter *et al.*, 1994]) and in pressure equilibrium with the surrounding plasma [cf. Burlaga and Lemaire 1978]. The electron population inside the hole may be affected in two ways: first, the adiabatic motion of the electrons (conservation of their magnetic momentum) passing through the hole along the magnetic field resulting in the filtering and focusing of the electrons and, second, time-of-flight effects associated with temporal variations in the properties of plasma entering the hole or nonstationarity of the hole itself. Because adiabatic focusing of thermal electrons by the hole will affect the electron temperature anisotropy, but hardly produce bimodal distributions or beamlike features, in a time stationary and symmetric situation (same electron distribution on both sides of the hole), some combination of both effects is required. Indeed, time-of-flight effects are well known to be responsible for reformation of electron beams in the fore-

shock [Filbert and Kellogg, 1979] or in type III solar bursts [Papadopoulos *et al.*, 1974]. Recent Vlasov simulations of generation of Langmuir waves by time-of-flight effects after a temporal change of electron distribution were performed by Briand *et al.* [2007].

[52] In the only published theoretical model for the formation of beams in magnetic holes proposed by MacDowall *et al.* [1996], the authors speculated that such a combination of adiabatic motion and time-of-flight effects acting on the thermal electron population could yield unstable distributions with the formation of two counterstreaming beams with velocities close to the electron thermal speed v_{te} . However these beams are not observed and would have hardly been unstable, as discussed above [Gary, 1985].

[53] The situation becomes significantly different if we take into account the suprathermal “strahl” component of the solar wind electron distribution, a field aligned population of electrons with speeds 3–10 times the electron thermal velocity and flowing along the field lines away from the Sun with a bulk speed larger than the solar wind velocity. The strahl electrons can thus penetrate the holes and provide a source population for the formation of electrons beams inside the magnetic holes.

[54] Indeed, we have shown in section 5.2, using Cluster data, that the occurrence of electrostatic waves inside magnetic holes is clearly associated with the presence of a significant strahl component in the ambient solar wind. We also show that the strahl inside the holes is weakened and dispersed in the holes. These observations suggest that the electrostatic waves are generated by electrons originating from the suprathermal strahl component. The formation of beams can be explained by a similar combination of adiabatic motion and time-of-flight effects as proposed by MacDowall *et al.* [1996] but applied to strahl electrons.

[55] As the strahl enters the hole due to its bulk flow velocity, its distribution is modified by two effects: (1) the adiabatic focusing described above and (2) particle drifts associated with magnetic field gradient and intrinsic electric field present inside the hole [Burlaga and Lemaire, 1978]. These two effects can drive the marginally stable distribution into an unstable state, resulting into wave excitation. This interpretation requires some level of fluctuations in the strahl component. The necessary electron beam can be formed from the fluctuating marginally stable strahl either directly by these effects (the strahl is also known to exhibit significant inhomogeneities and fluctuations on short time-scales [Louarn *et al.*, 2009]) or by time-of-flight effects.

[56] This interpretation appears to be consistent with previous studies on the occurrence of high-frequency waves and strahl in the fast and slow solar wind. Pilipp *et al.* [1987], Štverák *et al.* [2009], and others showed that the strahl is on average more intense in the fast solar wind. MacDowall *et al.* [2003] concluded that the relative occurrence of Langmuir waves inside magnetic holes is higher in the fast solar wind comparing to slow solar wind. While this agreement may be a simple coincidence, it is consistent with our results.

7. Summary and Conclusion

[57] In this article we performed a comprehensive experimental study of electrostatic wave activity localized inside

solar wind magnetic holes using new data from Cluster and STEREO spacecraft. These new data allowed us to identify properties of these waves and of the solar wind electron distribution with direct relevance to the yet unexplained mechanism of their generation.

[58] Concerning the waves, we have shown that (1) the absence of waves outside the holes proves their local formation. (2) High-frequency waves inside magnetic holes are largely electrostatic. They can be interpreted either as Langmuir waves, beam-mode waves (eigenmodes of plasma perturbed by the presence of a beam) or Z mode. (3) Fluctuations of the plasma peak frequency are observed between different short time wave packets forming individual TDS events as well as rather large variations of the polarization angle between such successive wave packets. These two points suggest that some kind of small scale magnetic or/and density fluctuations are present inside the holes.

[59] We have also provided new information about the particle distribution inside (through pitch angle distribution) and outside (skewness) the magnetic holes. In particular we have shown (i) a strong correlation between the presence of a strahl outside the hole and the presence of high-frequency wave inside the hole and (ii) a scattering of the electrons occur inside the hole, leading to an isotropization of the distribution function [also seen as an increase (decrease) of the perpendicular (parallel) temperature of the electrons].

[60] Based on these observations, we have provided a model for the excitation of the waves at the electron plasma frequency. The new aspect of this model compared to previous ones is to point to the importance of the strahl electrons for the generation of a bump in the electron distribution function.

[61] **Acknowledgments.** We thank the IMPACT team, and in particular Peter Schroeder, for the support with the MAG/IMPACT files. STEREO PLASTIC investigation (A.B. Galvin PI) and NASA contract NAS5-00132. We also thank B. Lavraud for his help with the Pitch Angle measurements of IMPACT/STEREO. IMPACT and PLASTIC data can be access through the STEREO Web site (http://stereo-ssc.nascom.nasa.gov/data/ins_data/). Part of the data analysis was done with the AMDA science analysis system provided by the Centre de Données de la Physique des Plasmas (CESR, Université Paul Sabatier, Toulouse) supported by the Centre National de la Recherche Scientifique and Centre National d'Études Spatiales. We thank the Cluster Active Archive and the instrument teams of the FGM, PEACE, Whisper, and WBD instruments of Cluster for the Cluster data used in this study. J.S. acknowledges the support of the grant 205/08/P129 of the Grant Agency of the Czech Republic.

[62] Philippa Browning thanks the reviewers for their assistance in evaluating this manuscript.

References

- Balogh, A., C. M. Carr, M. H. Acuña, M. W. Dunlop, T. J. Beek, P. Brown, et al. (2001), The Cluster Magnetic Field Investigation: Overview of in-flight performance and initial results, *Ann. Geophys.*, *19*, 1207–1217.
- Bougeret, J. L., et al. (2008), S/WAVES: The radio and plasma wave investigation on the STEREO Mission, *Space Sci. Rev.*, *136*, 487–528, doi:10.1007/s11214-007-9298-8.
- Briand, C., A. Mangeney, and F. Califano (2007), Electrostatic coherent structures generation by local heating in a collisionless plasma, *Phys. Lett. A*, *368*, 82–86, doi:10.1016/j.physleta.2007.03.077.
- Burlaga, L. F., and J. F. Lemaire (1978), Interplanetary magnetic holes: Theory, *J. Geophys. Res.*, *83*, 5157–5160, doi:10.1029/JA083iA11p05157.
- Burlaga, L. F., K. W. Ogilvie, and D. H. Fairfield (1969), Microscale fluctuations in the interplanetary magnetic field, *Astrophys. J.*, *155*, L171, doi:10.1086/180329.
- Burlaga, L. F., N. F. Ness, and M. H. Acuna (2007), Linear magnetic holes in a unipolar region of the heliosheath observed by Voyager 1, *J. Geophys. Res.*, *112*, A07106, doi:10.1029/2007JA012292.
- Buti, B., B. T. Tsurutani, M. Neugebauer, and B. E. Goldstein (2001), Generation mechanism for magnetic holes in the solar wind, *Geophys. Res. Lett.*, *28*, 1355–1358, doi:10.1029/2000GL012592.
- Cairns, I. H., P. A. Robinson, R. R. Anderson, and R. J. Strangeway (1997), Foreshock Langmuir waves for unusually constant solar wind conditions: Data and implications for foreshock structure, *J. Geophys. Res.*, *102*, 24,249–24,264, doi:10.1029/97JA02168.
- Cummings, W. D., and P. J. Coleman Jr. (1968), Magnetic fields in the magnetopause and vicinity at synchronous altitude, *J. Geophys. Res.*, *73*, 5699–5718, doi:10.1029/JA073i017p05699.
- Décrou, P., P. Fergau, V. Krasnoselskikh, et al. (1997), Whisper, a resonance sounder and wave analyser: Performances and perspectives for the Cluster mission, *Space Sci. Rev.*, *79*, 157–193.
- Feldman, W. C., J. R. Asbridge, S. J. Bame, M. D. Montgomery, and S. P. Gary (1975), Solar wind electrons, *J. Geophys. Res.*, *80*, 4181–4196.
- Filbert, P. C., and P. J. Kellogg (1979), Electrostatic noise at the plasma frequency beyond the earth's bow shock, *J. Geophys. Res.*, *84*, 1369–1381, doi:10.1029/JA084iA04p01369.
- Fränz, M., D. Burgess, and T. S. Horbury (2000), Magnetic field depressions in the solar wind, *J. Geophys. Res.*, *105*, 12,725–12,732, doi:10.1029/2000JA900026.
- Galvin, A. B., et al. (2008), The Plasma and Suprathermal Ion Composition (PLASTIC) Investigation on the STEREO observatories, *Space Sci. Rev.*, *136*, 437–486, doi:10.1007/s11214-007-9296-x.
- Gary, S. P. (1985), Electrostatic instabilities in plasmas with two electron components, *J. Geophys. Res.*, *90*, 8213–8221.
- Gurnett, D. A., R. L. Huff, and D. L. Kirchner (1997), The wide-band plasma wave investigation, *Space Sci. Rev.*, *79*, 195–208.
- Henri, P., C. Briand, A. Mangeney, S. D. Bale, F. Califano, K. Goetz, and M. Kaiser (2009), Evidence for wave coupling in type III emissions, *J. Geophys. Res.*, *114*, A03103, doi:10.1029/2008JA013738.
- Johnstone, A. D., et al. (1997), PEACE: A plasma electron and current experiment, *Space Sci. Rev.*, *79*, 351–398.
- Lin, N., P. J. Kellogg, R. J. MacDowall, A. Balogh, R. J. Forsyth, J. L. Phillips, A. Buttighoffer, and M. Pick (1995), Observations of plasma waves in magnetic holes, *Geophys. Res. Lett.*, *22*, 3417–3420, doi:10.1029/95GL03266.
- Lin, N., P. J. Kellogg, R. J. MacDowall, B. T. Tsurutani, and C. M. Ho (1996), Langmuir waves associated with discontinuities in the solar wind: A statistical study, *Astron. Astrophys.*, *316*, 425–429.
- Louarn, P., et al. (2009), On the temporal variability of the “Strahl” and its relationship with solar wind characteristics: STEREO SWEA observations, *Sol. Phys.*, *259*, 311–321.
- Luehr, H., and N. Kloecker (1987), AMPTE-IRM observations of magnetic cavities near the magnetopause, *Geophys. Res. Lett.*, *14*, 186–189, doi:10.1029/GL014i003p0186.
- Luhmann, J. G., et al. (2008), STEREO IMPACT investigation goals, measurements, and data products overview, *Space Sci. Rev.*, *136*, 117–184, doi:10.1007/s11214-007-9170-x.
- MacDowall, R. J., N. Lin, P. J. Kellogg, A. Balogh, R. J. Forsyth, and M. Neugebauer (1996), Langmuir waves in magnetic holes: Source mechanism and consequences, in *Solar Wind Eight: Proceedings of the Eighth International Solar Wind Conference*, edited by D. Winterhalter et al., *AIP Conf. Proc.*, *382*, 301–304.
- MacDowall, R. J., R. A. Hess, N. Lin, and G. Thejappa (1997), Plasma wave observations from the ULYSSES spacecraft's fast heliographic latitude scan, *Adv. Space Res.*, *19*, 873–876, doi:10.1016/S0273-1177(97)00295-0.
- MacDowall, R. J., N. Lin, and D. J. McComas (2001), Langmuir wave activity: Comparing the Ulysses solar minimum and solar maximum orbits, *Space Sci. Rev.*, *97*, 141–146, doi:10.1023/A:1011846700852.
- MacDowall, R. J., N. Lin, and D. J. McComas (2003), Heliospheric Langmuir wave observations from the Ulysses spacecraft, *Adv. Space Res.*, *32*, 479–483, doi:10.1016/S0273-1177(03)00331-4.
- Montgomery, M. D., S. J. Bame, and A. J. Hundhausen (1968), Solar wind electrons: Vela 4 measurements, *J. Geophys. Res.*, *73*, 4999–5003, doi:10.1029/JA073i015p04999.
- Muschietti, L., I. Roth, and R. Ergun (1994), Interaction of Langmuir wave packets with streaming electrons: Phase-correlation aspects, *Phys. Plasmas*, *1*, 1008–1024, doi:10.1063/1.870781.
- Neugebauer, M., B. E. Goldstein, D. Winterhalter, E. J. Smith, R. J. MacDowall, and S. P. Gary (2001), Ion distributions in large magnetic holes in the fast solar wind, *J. Geophys. Res.*, *106*, 5635–5648, doi:10.1029/2000JA000331.
- Papadopoulos, K., M. L. Goldstein, and R. A. Smith (1974), Stabilization of electron streams in Type III solar radio bursts, *Astrophys. J.*, *190*, 175–186, doi:10.1086/152862.
- Pilipp, W. G., K.-H. Muehlhaeuser, H. Miggenrieder, M. D. Montgomery, and H. Rosenbauer (1987), Characteristics of electron velocity distribu-

- tion functions in the solar wind derived from the HELIOS plasma experiment, *J. Geophys. Res.*, *92*, 1075–1092.
- Russell, C. T., W. Riedler, K. Schwingenschuh, and Y. Yeroshenko (1987), Mirror instability in the magnetosphere of Comet Halley, *Geophys. Res. Lett.*, *14*, 644–647, doi:10.1029/GL014i006p00644.
- Sauvaud, J.-A., et al. (2008), The IMPACT Solar Wind Electron Analyzer (SWEA), *Space Sci. Rev.*, *136*, 227–239, doi:10.1007/s11214-007-9174-6.
- Stevens, M. L., and J. C. Kasper (2007), A scale-free analysis of magnetic holes at 1 AU, *J. Geophys. Res.*, *112*, A05109, doi:10.1029/2006JA012116.
- Štverák, Š., M. Maksimovic, P. M. Trávníček, E. Marsch, A. N. Fazakerley, and E. E. Scime (2009), Radial evolution of nonthermal electron populations in the low-latitude solar wind: Helios, Cluster, and Ulysses Observations, *J. Geophys. Res.*, *114*, A05104, doi:10.1029/2008JA013883.
- Treumann, R. A., N. Sckopke, L. Brostrom, and J. Labelle (1990), The plasma wave signature of a ‘magnetic hole’ in the vicinity of the magnetopause, *J. Geophys. Res.*, *95*, 19,099–19,114, doi:10.1029/JA095iA11p19099.
- Tsurutani, B. T., B. Dasgupta, C. Galvan, M. Neugebauer, G. S. Lakhina, J. K. Arballo, D. Winterhalter, B. E. Goldstein, and B. Buti (2002), Phase-steepened Alfvén waves, proton perpendicular energization and the creation of magnetic holes and magnetic decreases: The ponderomotive force, *Geophys. Res. Lett.*, *29*(24), 2233, doi:10.1029/2002GL015652.
- Turner, J. M., L. F. Burlaga, N. F. Ness, and J. F. Lemaire (1977), Magnetic holes in the solar wind, *J. Geophys. Res.*, *82*, 1921–1924, doi:10.1029/JA082i013p01921.
- Winterhalter, D., M. Neugebauer, B. E. Goldstein, E. J. Smith, S. J. Bame, and A. Balogh (1994), ULYSSES field and plasma observations of magnetic holes in the solar wind and their relation to mirror-mode structures, *J. Geophys. Res.*, *99*, 23,371–23,381.
- Winterhalter, D., M. Neugebauer, B. E. Goldstein, E. J. Smith, B. T. Tsurutani, S. J. Bame, and A. Balogh (1995), Magnetic h in the solar wind and their relation to mirror mode structures, *Space Sci. Rev.*, *72*, 201–204, doi:10.1007/BF00768780.
- Yoon, P. H., L. F. Ziebell, and C. S. Wu (2000), Excitation of Langmuir waves in interplanetary space, *J. Geophys. Res.*, *105*, 27,369–27,376, doi:10.1029/2000JA000230.
- Zhang, T. L., et al. (2008), Characteristic size and shape of the mirror mode structures in the solar wind at 0.72 AU, *Geophys. Res. Lett.*, *35*, L10106, doi:10.1029/2008GL033793.
- Zurbuchen, T. H., et al. (2001), On the origin of microscale magnetic holes in the solar wind, *J. Geophys. Res.*, *106*, 16,001–16,010, doi:10.1029/2000JA000119.

C. Briand, P. Henri, and A. Mangeney, LESIA, Observatoire de Paris, CNRS, UPMC, Université Paris Diderot, 5 place J. Janssen, F-92190 Meudon, France.

J. Soucek, Department of Space Physics, Institute of Atmospheric Physics, ASCR, CZ-14131 Prague, Czech Republic.